THE SOLID STATE SPECTROSCOPY OF POLY-5,5'-(4-4'-DINONYL-2,2'BITHIAZOLE); FROM OLIGOMERS TO POLYMER

W.M. Blanda, A.H. Francis and M.D. Curtis

Department of Chemistry
University of Michigan
930 N. University
Ann Arbor, Mi. 48104

Introduction

Polymers with extended conjugation along the backbone are typically referred to as conducting polymers and their electronic structure suggests their suitability for use in a variety of semiconductor devices[1]. However, the potential utility of conducting polymers in device technology depends not only on the π-delocalization of the molecule, but also on a variety of solid state interactions that affect the conductivity of the polymer material. Therefore, when designing π-conjugated polymers for semiconductor applications, it is important to understand both inter- and intramolecular electronic effects[2]. In order to gain a better understanding of the role of these effects in mediating charge transport in π-conjugated polymers, we have carried out a spectroscopic study of a polymer designed to have a planar, π-conjugated backbone geometry and a well-defined intermolecular packing arrangement. In order to aid in the interpretation of the spectroscopic data, we have also examined the spectra of the monomeric precursor, (4-4'-dinonyl-2,2'bithiazole)5,5'-diyl (P4NonTz, Figure 1), as well as a number of oligiomers. Spectra have been obtained from samples isolated in dilute solution and also in the solid state.

© WILEY-VCH Verlag GmbH, D-69469 Weinheim, 2000 CCC 1022-1360/00/$ 17.50+.50/0

Previous publications have addressed the crystalline packing and the optical properties of P4NonTz[3], also referred to as PNBT[4]. Like CN-PPV[5], this polymer also has a cofacial crystalline packing structure, with an interplanar distance less than four angstroms[6]. This same packing structure is seen in the oligomers[7]. Other properties that are common to conducting polymers, such as solvatochromism, nonlinear optical properties, and redox potentials have also been noted[8]. However, minimal information on the most basic structures, the oligomers, has been utilized thus far to extrapolate properties of the polymer.

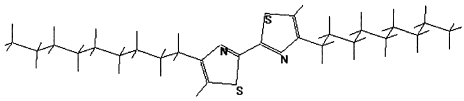

Figure 1. (4-4'-dinonyl-2,2'bithiazole)5,5'-diyl

Experimental

Materials. The preparation of the oligomers and polymer, via a zerovalent nickel complex and subsequent Stille coupling, has been reported elsewhere[9].

Instrumentation. Oligomers and polymer were dissolved in toluene and stirred at 80^0C for 10 minutes and subsequently diluted to produce solutions with concentrations no greater than $4x10^{-5}$ M. Solid state spectra were produced from powder samples as precipitated from MeOH in the synthesis process, or from films cast from toluene.

The UV-VIS absorption spectra were taken with a Shimadzu UV160U UV-visible recording spectrophotometer, which uses a double beam for background corrections. Emission and excitation spectra were recorded with a Horiba group Instruments S.A. Inc. FluoroMax-2 spectrofluorimeter. This contained an ozone-free 150W Xenon lamp and a model 96455 photomultiplier tube that was sensitive from 200-900nm. All spectra were corrected for lamp intensity and PMT response by using Datamax software.

Emission spectra at cryogenic temperatures were acquired by using an Osram xenon arc lamp with a $CuSO_4$ filter, and the proper combination of Corning filters to select the range of wavelengths that roughly corresponded to the absorbance maximum of the sample. The light was then focused on the sample in the Janus cryostat, and a Corning filter was used to pass emission wavelengths at 90 degrees from the incident beam. The signal was chopped at 100 Hz, passed through an Arc Spectra-Pro-275 scanning monochromator, and amplified with a Hammamatsu 375 photomultiplier tube. A PAR 126 lock-in amplifier was used in conjunction with a Keithley model 575 interface to improve and digitize the signal.

Calculations. Electronic transition energies and oscillator strengths were computed for each of the oligiomeric species. The molecular geometry of each oligiomer was first optimized using the MINDO3 semiempirical method with the oligiomer's structure constrained to the planar, trans configuration. Subsequently, the electronic spectra were calculated using the ZINDO-S semiempirical method, including interactions between singly-excited configurations involving the first three occupied and unoccupied molecular orbitals.

Results and Discussion

Spectroscopy. The absorption, excitation and emission spectra of 4,4'-dinonyl-2,2'bithiazole monomer, dimer, trimer, pentamer, and polymer in toluene solution are collected and compared in **Figure 1**. The excitation spectra were recorded by monitoring the corresponding emission maxima, and the emission spectra were obtained by exciting at the frequency of the corresponding absorption maxima. There is a close correspondence between the absorption spectrum and the corresponding excitation spectrum, suggesting that the emission observed is characteristic of the bulk sample, and not attributable to a small concentration of chemical impurity (e.g. other oligiomeric species or monomer). The absorption spectra shift progressively to lower energy with increasing chain length, suggesting that the correlation between chain length and π-electron delocalization is preserved throughout the oligiomer sequence. The emission spectra exhibit a large Stokes shift (~5000 cm^{-1}), which is indicative of a substantial change in molecular geometry or solvent interactions upon electronic

excitation of the π-conjugated backbone. This behavior is typical of large π-conjugated molecules.[10]

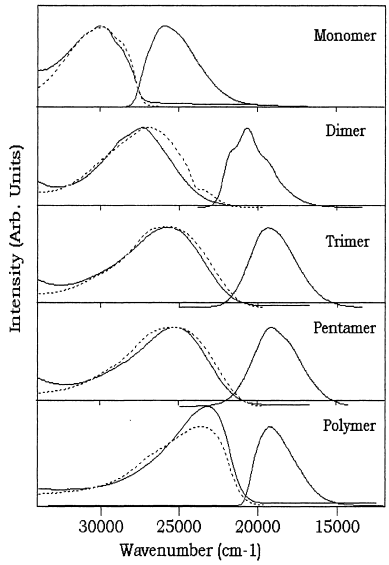

Figure 2. Absorbance, excitation(dashed) and emission of monomer, dimer, trimer, tetramer, and pentamer in toluene.

The solid-state absorption, emission and excitation spectra of the samples are collected in Figure 3. With the exception of the monomer, all of the solid-state spectra are displaced to lower energy relative to the corresponding solution spectra. The solid-state absorption spectra exhibit a weak feature corresponding to the solution absorption maximum. This indicates the presence of a small concentration of isolated oligiomer, with intermolecular interactions and molecular configurations typical of those in solution. The principal features of the absorption spectra are considerably shifted to lower energy. The magnitude of the shift results from strong intermolecular interactions that are enabled by the co-planar, π-stacked arrangement of the oligomers that characterizes the bulk of the sample.

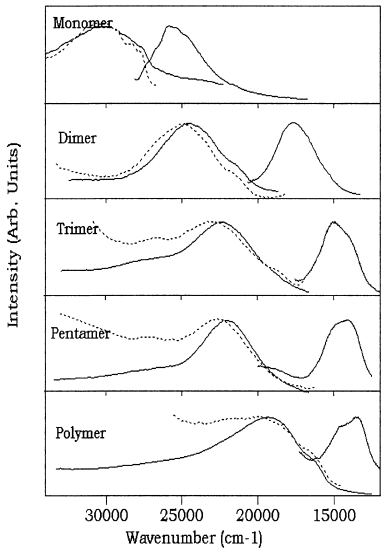

Figure 3. Solid state absorbance, excitation(dashed) and emission of monomer, dimer, trimer, pentamer, and polymer.

Both the absorption and emission spectra of crystalline monomer 4NonTz, recorded at 4K exhibit a well-resolved vibronic structure (see Fig. 7). At 4 K, the electronic origin of the emission spectrum falls slightly to lower energy of the absorption origin signaling that the emission spectrum arises from shallow defects. At 77 K, thermal population of the bulk states produces an emission spectrum whose origin is coincident with that of the absorption spectrum. The vibronic envelopes of the absorption and emission spectra are consistent with those expected for an electric-dipole allowed excitation, accompanied by a relatively large change in molecular geometry (e.g. a Franck-Condon forbidden excitation). Both the large oscillator strength of the transition (see below, Fig. 7) and the substantial Stokes loss observed throughout the oligiomer sequence are consistent with this conclusion.

The Franck-Condon active vibrations in the spectra of the monomer are easily identified. In the absorption spectrum there is a clear origin, and a progression interval of approximately 700 cm^{-1} that we assign to a C-S stretching mode. A 1650 cm^{-1} interval that may correspond to either a C=C stretch, or a C=N stretch, is observed in combination with the C-S stretch. The vibronic activity in the emission

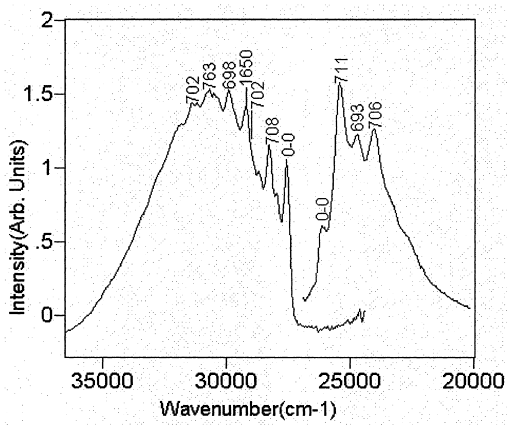

Figure 4. Absorption and emission of 4NonTz monomer crystals at 4K

spectrum correlates well with that of the absorption spectrum and there exists an approximate "mirror image" symmetry between the respective vibronic envelopes. The vibronic activity observed in the absorption and emission spectra of monomer is consistent with the increased antibonding electron population that accompanies the $\pi^* \leftrightarrow \pi$ excitation. The LUMO orbital exhibits a nodal plane transecting the C-S and C-C bonds. Accordingly, the $\pi^* \leftrightarrow \pi$ excitation is expected to produce a lengthening of these bonds and a general increase in the size of the thiazole ring.

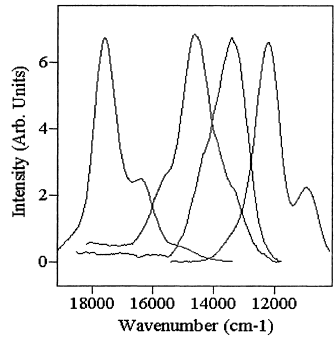

Figure 5. Solid state emission spectra at 77K of (left to right) dimer, trimer, pentamer, and polymer.

The low-temperature emission spectra of the dimer, trimer, pentamer, and polymer (shown in Fig. 5) exhibit less resolved vibronic structure than the monomer. In general, the spectra seem to be composed of three poorly resolved bands. It is of interest that these features of the spectral envelope appear to be characteristic of many planar, conjugated polymers, and have been attributed to the presence of different conjugation lengths in the polymeric sample[11], to vibronic transitions[12], and to aggregation[13].

Theoretical Calculations. The experimental transition energy is compared with theoretical predictions in Figure 6 where the calculated (ZINDO/S) and observed energy of the absorption maximum is plotted as a function of reciprocal chain length (n=number of monomer units). A nearly linear relationship is both predicted and observed. The linear dependence is also predicted by a simple free electron model (eq. 2 with DB=4n).

The calculated oscillator strength and experimental molar absorptivity of the oligiomers and the polymer of 4NonTz are compared in Figure 7. Eq. (1) gives the well known free electron molecular orbital theory prediction for the one-electron oscillator strength, where DB is the number of double bonds along the conjugated backbone. For modest values of DB a linear relationship between DB and the oscillator strength is predicted[14]. The calculated oscillator strengths, shown in Figure 7, display the same linear trend as the experimental molar absorptivities.

$$f_1 \propto \frac{8}{3\pi^2} * \frac{DB^2(DB+2)^2}{(DB+1)^3} \approx \frac{8}{3\pi^2} * DB \qquad (1)$$

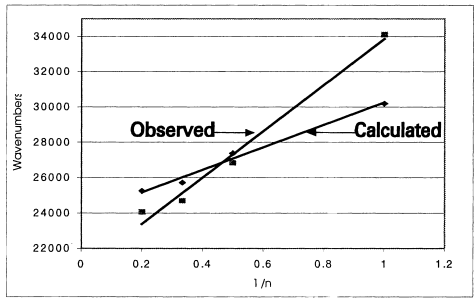

Figure 6. Experimental and calculated absorbance maxima vs. number of bithiazole units(n)

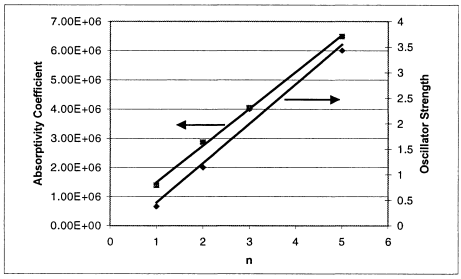

Figure 7. Number of bithiazole units (n) vs. observed molar absorptivity coefficient and calculated electric dipole moment.

The oligomers are expected to exhibit a delocalized π-electronic structure along the conjugated backbone. In this regard, the polythiazoles are similar to many other π-conjugated polymers, the closest correspondence being to the more extensively studied polymer of thiophene. There are two important chemical and structural aspects to consider when discussing the polythiazoles: the introduction of a nitrogen heteroatom into the polymer backbone, and the alkyl sidechains.

The single most important effect of the heteroatom is to induce an alternation in the bond lengths and an increase the fluctuation of the potential experienced by an π-electron accelerated along the polymer backbone. The alkyl substituent side chains are expected to have a substantial effect on the equilibrium structure of the backbone and on the crystal packing arrangement.

A simple free electron model of the π-conjugated backbone leads to the well known result for the energy of the homo-lumo (or bandgap) transition of a polymer containing DB equivalent double bonds, each of length a, where L

$$\Delta E = \frac{h^2}{8mL^2}(2DB+1) \approx \frac{h^2}{16ma^2} * (\frac{1}{DB}) \qquad (2)$$

is the polymer overall length and m is the mass of the electron. Eq. 2 predicts a linear variation of the homo-lumo energy difference with 1/DB that extrapolates to zero at infinite chain length. This model works for cyanine dyes, but fails (for example) in

the case of polyenes, because of a small, but significant alternation in bond lengths along the polymer chain. The potential fluctuation along the chain results in a modification of Eq. 3, first derived by

$$\Delta E = \frac{h^2}{8mL^2}(2DB+1) + V_0(1-\frac{1}{2DB}) \qquad (3)$$

Kuhn,[15] where V_0 is the amplitude of the potential fluctuation. The extended free electron model also predicts a linear variation of the homo-lumo energy difference with 1/DB, but extrapolates to V_0 at infinite chain length. A comparison of the homo-lumo gap for several polymers in Figure 8 illustrates a fundamental difference between the polyenes, poly-thiophenes and poly- thiazoles. The inclusion of the nitrogen hetero-atom in the poly-thiazoles results in the opening of a substantially larger bandgap (V_0) in these polymers than is observed in the polyenes or the poly-thiophenes.[16]

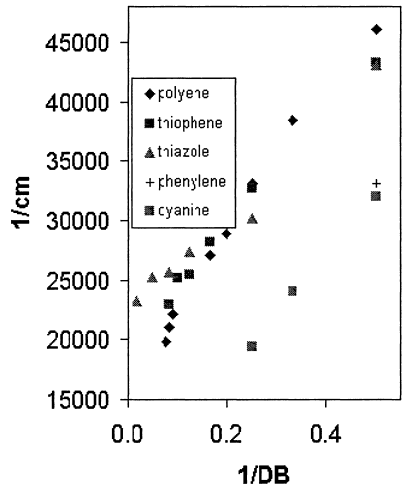

Figure 8. Band gap vs. 1/number of double bonds for polyenes, polythiophenes, and polythiazoles.

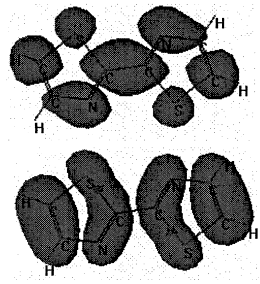

Figure 9. Calculated HOMO (lower) and LUMO (upper) for P4NonTz

When the HOMO and LUMO orbitals associated with the band-gap excitation are examined using MINDO3, the electron density maps shown in Figure 9 are obtained. These reveal substantial changes in the C-S, C=N and C=C bond orders upon electronic excitation and are consistent with the vibronic activity observed in the electronic spectrum. The substantial in-plane distortions of the thiazole rings along the conjugated backbone are likely responsible for the large Stokes loss observed in the spectra of the oligiomer and polymer samples. Since the distortions are predicted to involve only in-plane motions, the conjugation along the backbone remains largely undisturbed by electronic excitation.

Conclusion

The electronic absorption and emission spectra of a series of oligothiazoles with well-defined backbone geometries have been examined in order to better understand aspects of inter- and intra-molecular interactions on the extent of π-conjugation. For this purpose, comparisons between the spectra obtained from solutions and those from solid-state samples are particularly useful.

The absorption and emission spectra of both solution and solid-state samples exhibit a shift to lower energy with an increasing number of bithiazole units. This observation is in agreement with the predictions of ZINDO-S calculations, as well as free-electron molecular orbital theory. The spectral results are similar to those established for other

conjugated polymers, yet take on individual characteristics that can be explained by the alternation of the electronic potential caused by the nitrogen heteroatom.

The solid-state spectra of the oligiomers and the polymer are strongly red shifted relative to the solution spectra, and exhibit spectral envelopes composed of 2 or 3 poorly resolved bands. Similar features have been observed in the spectra of other conjugated polymers and variously interpreted. These features may either be intermolecular (excimer, aggregate, charge-transfer complex, etc.) or molecular (vibronic, a distribution of conjugation lengths) in origin. The relatively short interplanar distance (3.7Å) is conducive to excimer formation and the large apparent Stokes loss is consistent with this process. However, excimer emission is typically broad and featureless, whereas this emission contains multiple maxima that are significantly sharper than observed in the spectra of the isolated molecule.

On the other hand, the emission is not sufficiently sharp to be attributed to J- or H-type aggregates. Moreover, aggregates of this type give rise to strong, nearly coincident, absorption and emission bands. This is not observed in the spectra of the oligomers and the polymer.

The tendency of the oligiomers and the polymer to form π-stacks in a coplanar arrangement may lead to the appearance of structure in the electronic spectrum. Strong coupling within a π-stack and/or between different π-stacks can produce additional structure in the electronic spectrum. The effect is similar to exciton or factor group splitting that is commonly observed in many crystalline solids and is dependent on the number of molecules per unit cell and the intermolecular coupling.

We believe that the structure observed in the spectra of the oligomers is neither vibronic nor conformational in origin. Although the energy intervals between these features are approximately the same as a vibrational interval, the relative intensities of these features are sensitive to sample handling. This result is inconsistent with vibronic structure. The number of conformations for small molecules is limited. If the multiple features were attributed to conformations, a shorter oligomer should exhibit fewer features. As seen in figure 5, the dimer and the polymer have almost identical features.

It is our view that the structure observed in the emission spectra of the oligomers and the polymer is most likely the result of intermolecular interactions and that such

interactions are promoted by the tendency of planar, π-conjugated polymers to π-stack.

References

1 Gonzalez Ronda, L.; Martin, D. C., *Macromolecules*, **1997**, *30*, 1524-1526.

2 Politis, J.K.; Curtis, M.D.; Gonzales Ronda, L.; Martin, D.C. He, Y.; Kanicki, J.; *Chem. Mater.*, **1998**, *10*, 1713.

3 Conwell, E.M.; Perlstien, J.; Shaik, S.; *Phys. Rev. B*, **1996**, 54(4), 2308-2310.

4 Yamamoto, T.; Komarudin, D.; Arai, M.; Lee, B.; Saganuma, H.; Asakawa, N.; Inoue, Y.; Kubota, K.; Sasaki, S.; Fukuda, T.; Matsuda, J.; *J. Am. Chem. Soc.*, **1998**, *120*, 2047-2058.

5 Curtis, M.D.; Blanda, W.M.; Politis, J.K.; Francis, A.H.; Lee, J.; Kampf, J; Gondalez-Ronda, L.; Martin, D.C.; *Proc. Mat. Res. Soc.*, **1998,** *to be published.*

6 Yamamoto, T.; Suganuma, H.; Maruyama, T.; Inoue, T.; Muramatsu, Y.; Minoru, A.; Komarudin, D.; Ooba, N.; Tomaru, S.; Sasaki, S.; Kubota, K.; *Chem. Mater.*, **1997**, 1217-1225.

7. Nanos, J.I.; Kampf, J.W.; Curtis, M.D.; Gonzales, L.; Martin, D.C.;*Chem.Mater*, **1995**, 7.

8 Hide F.; Schwartz B.J.; Diaz-Garcia M.A.; Heeger A.J., *Synth Met*, **1997**, *91*, 35-40.

9 (a)Mc Cullough, R. D.; Tristram-Nagle, S.; Williams, S.P.; Jayaraman, M.; *J. Am. Chem. Soc.*, **1993**, *115*, 4910. (b) Sandstedt, C.A.; Rieke, R.D.; Eckhardt, C. J.; *Chem. Mater.* **1995**, *7*, 1057-1059. (c)Yang, C.; Orfino, F.P.; Holdcroft, S.; *Macromolecules* **1996**, *29*, 6510. (d) Park, K. C.; Levon, K.; *Macromolecules* **1997**, *30*, 3175.

10 (a)Danno, T.; Kuerti, J.; Kuzmany, H.; *Front. Polym. Res.,[Proc. Int. Conf.]*, 1st, 219-222. Edited by: Prasad, P.N.; Nigam, J.K. Plenum; New York 1991, N.Y. (b) Yamamoto, T.; Honda, K.; Ooba, N.; Tomaro, S.; *Macromolecules*, **1998**, *31*,7.

11 (a)Yamamoto, T.; Komarudin, D.; Arai, M.; Lee, B.; Suganuma, H.; Asakawa, N.; Inoue, Y.; Kubota, K.; Sasaki, S.; Fukuda, T.; Matsuda, H.; *J. Am. Chem. Soc.***1998**, *120*, 2047. (b)Halkyard, C.E.; Rampey, M. E.; Koppenburg, L.; Studer-Martinez, S. L.; Bunz, U. H. F.; *Macromolecules* **1998**, *31*, 8655. (c) Langeveld-Voss, B. M. W.; Janssen, R. A. J.; Christiaans, M. P. T.; Meskers, S. C. J.; Dekkers, H. P. J. J.; Meijer, E. W.; *J. Am. Chem. Soc.* **1996**, *118*, 4908. (d) Langeveld-Voss, B. M. W.; Waterval, R. J. M.; Janssen, R. A. J.; Meijer, E. W.; *Macromolecules* **1999**, *32*, 227.

12 Jaffe, H. H.; Orchin, M.; Theory and Applications of Ultraviolet Spectroscopy, Wiley and Sons, 1964.

13 Kuhn, Hans *J.Chem.Phys.*, **1949**, 17, 1198.

14 Bredas J. L.; Sibley R.; Boudreaux D. S.; Chance R. R. *J. Am. Chem. Soc.*, **1983**, 105, 6555-6559.